Biochemical and Biophysical Research Communications **269,** 131–136 (2000)
doi:10.1006/bbrc.2000.2254, available online at http://www.idealibrary.com on IDEAL®

Chemiluminescent Detection and Imaging of Reactive Oxygen Species in Live Mouse Skin Exposed to UVA

Hiroyuki Yasui and Hiromu Sakurai[1]

Department of Analytical and Bioinorganic Chemistry, Kyoto Pharmaceutical University, 5 Nakauchi-cho, Misasagi, Yamashina-ku, Kyoto 607-8414, Japan

Received January 14, 2000

The recent increase of ultraviolet (UV) rays on Earth due to the increasing size of the ozone hole is suggested to be harmful to life and to accelerate premature photoaging of the skin. The detrimental effects of UV radiation on the skin are associated with the generation of reactive oxygen species (ROS) such as superoxide anion radical ($^{\cdot}O_2^-$), hydrogen peroxide (H_2O_2), hydroxyl radical ($^{\cdot}OH$), and singlet oxygen ($^1O_2$). However, direct proof of such ROS produced in the skin under UV irradiation has been elusive. In this study, we report first *in vivo* detection and imaging of the generated ROS in the skin of live mice following UVA irradiation, in which both a sensitive and specific chemiluminescence probe (CLA) and an ultralow-light-imaging apparatus with a CCD camera were used. In addition, we found that $^{\cdot}O_2^-$ is formed spontaneously and $^1O_2$ is generated in the UVA-irradiated skin. This method should be useful not only for noninvasive investigation of the spatial distribution and quantitative determination of ROS in the skin of live animals, but also for *in vivo* evaluation of the protective ability of free radical scavengers and antioxidants.

Key Words: **chemiluminescent detection; ultralow-light imaging; UV irradiation; reactive oxygen species (ROS); superoxide anion radical ($^{\cdot}O_2^-$); singlet oxygen ($^1O_2$); live mice skin.**

The ozone shield prevents sunlight from reaching the surface of the Earth and protects animals and plants from excessive exposure of ultraviolet (UV) rays. Global air pollution by chemical compounds such as fluorocarbons causes ozone shield depletion and results in increases in UV radiation (1, 2). Since the surface of human skin is affected by many surrounding environmental factors such as solar light, recent increases in UVB (280–320 nm) and UVA (320–400 nm) radiation have been assumed to enhance damage and to induce premature aging in human skin. UVA rays penetrate more deeply into the dermal matrix of the skin tissue than do UVB rays (3, 4), and UVA rays have been reported to contribute particularly to the development of both photoaging skin (5, 6), which is characterized by deep wrinkles and severe pigmentation, and skin cancer (7).

Previously demonstrated evidence has suggested that the harmful effects of UV radiation on the skin are related to the generation of reactive oxygen species (ROS) such as superoxide anion radical ($^{\cdot}O_2^-$), hydrogen peroxide (H_2O_2), hydroxyl radical ($^{\cdot}OH$), and singlet oxygen ($^1O_2$). Homogenized epidermis exposed to UV irradiation has been seen to generate $^{\cdot}O_2^-$, as detected by the ESR-spin trapping method (8). H_2O_2 and $^{\cdot}OH$ have been detected in cultured murine skin fibroblasts exposed UVB, using fluorescent rhodamine 123 and ESR-spin trapping, respectively (9, 10). The cytotoxicity of cultured human skin fibroblasts after UVA irradiation was dependent on the endogenous production of $^1O_2$ in the cell (11, 12). ROS scavenging enzymes such as superoxide dismutase (SOD), catalase (CAT), and glutathione peroxidase (GSH-Px) have been shown to prevent cell sunburn induced by UV exposure (13, 14), and decomposition of collagen and hyaluronic acid as the constituents of proteoglycans were observed to be promoted by $^{\cdot}OH$ in *in vitro* studies (15). Oxidative stresses such as the depletion of glutathione, induction of lipid peroxidation, and hydroperoxidation of cholesterol were extensively found in UV-ray-exposure sites of *in vivo* mouse or rat skin (16, 17).

Abbreviations used: ROS, reactive oxygen species; UVA, ultraviolet light A; CL, chemiluminescence; $^{\cdot}O_2^-$, superoxide anion radical; $^1O_2$, singlet oxygen species; H_2O_2, hydrogen peroxide; $^{\cdot}OH$, hydroxyl radical; CLA, *Cypridina hilgendorfii* luciferin analog; 2-methyl-6-phenyl-3;7-dihydroimidazo [1,2-*a*] pyrazine-3-one; SOD, superoxide dismutase; CAT, catalase; GSH-Px, glutathione peroxidase; DFO, deferoxamine.

[1] To whom correspondence should be addressed. Fax: 81-75-595-4753. E-mail: sakurai@mb.kyoto-phu.ac.jp.

0006-291X/00 $35.00

Although many such findings have been reported, direct proof of ROS generated by UV irradiation in the *in vivo* skin has yet been elusive. Therefore, the detection and identification of ROS on skin under UV exposure are highly important for discussing the previously proposed role of ROS in the photoaging of human skin. However, very little research has been conducted so far measuring ROS in human subjects. In only two reports, a human forearm and a hairless mouse were used to evaluate the occurrence of ROS in skin exposed to UVA radiation (18, 19). The methods and technical systems used in those studies were specially developed for measuring *in vivo* ultraweak photon emission (UPE) or low-level chemiluminescence in human and mouse skin (18, 19). The effectiveness of topically applied antioxidants such as α-tocopherol, β-carotene, and α-glucosylrutin (flavonoid) on the skin exposed to UVA radiation was also evaluated in these studies.

$^{\cdot}O_2^-$ and $^1O_2$, which are generated by the one-electron reduction and excitation of molecular dioxygen, respectively, have been of great interest in the fields of biochemistry and medicine. At present, it is very difficult to present evidence for the occurrence and quantitative distribution of $^{\cdot}O_2^-$ and $^1O_2$ in an entire living body because the concentration of $^{\cdot}O_2^-$ and $^1O_2$ formed *in vivo* is very low, leaving a short half-life in an aqueous system, i.e., 50 msec for $^{\cdot}O_2^-$ and 2–5 μsec for $^1O_2$ (20–22). In our laboratory, ROS has been detected by various methods such as chemiluminescence (CL), electron spin resonance (ESR), and UV–VIS spectroscopy in *in vitro* systems (9, 10, 23–28). Among them, the CL detection technique using a CL probe, which is followed by little interference with other factors and nontoxicic to the systems, is more sensitive than other methods. Highly sensitive and specific CL probes for $^{\cdot}O_2^-$ and $^1O_2$, *Cypridina hilgendorfii* luciferin analogs, have been developed by Goto and co-workers (29–31) and widely used in the studies of $^{\cdot}O_2^-$ and $^1O_2$ in chemical and biological systems (32–35).

A new photon-imaging instrumentation such as ultrasensitive luminographs taken by CCD cameras has been developed in parallel with improvements in CL probes. The sensitivity and spatial resolution of modern peltier-air-cooled CCD cameras, which provide improved sensitivity, dynamic range, excellent image quality and robustness, have resulted in a variety of new applications in the life sciences (36, 37). These instruments employing a new generation of cooled CCD cameras display quantitative localization of the CL signals with adequate spatial resolution on a targeted surface such as tissues, as well as provide quantification at the level of a single photon due to low-level CL (38, 39).

Under these conditions, we tried to detect and identify ROS generated in the skin of live mice exposed to UVA light, in which a new method utilizing both the sensitive and specific CL probe and ultralow-light-imaging apparatus with a CCD camera was used for the *in vivo* detection and imaging of ROS identified as $^{\cdot}O_2^-$ and $^1O_2$.

MATERIALS AND METHODS

Materials. Male ddy mice (6–8 weeks old) weighing about 30 g were purchased from Shimizu Experimental Materials (Kyoto, Japan). *Cypridina hilgendorfii* luciferin analog, 2-methyl-6-phenyl-3,7-dihydroimidazo-[1,2-*a*]pyrazin-3-one (CLA), and β-carotene were obtained from Tokyo Kasei Organic Chemicals (Tokyo, Japan). Phenobarbital sodium was from Maruko (Nagoya, Japan). Superoxide dismutase (SOD) and catalase (CAT) were obtained from Sigma (St. Louis, MO). Deferoxamine (DFO) was purchased from Takeda Pharmaceutical (Osaka, Japan). Black cloth made of a synthetic fiber was from Nomura Tailor (Kyoto, Japan). All other chemicals were of high-quality analytical grade.

Ultralow-light imaging system. The luminograph used (the new NightOWL Molecular Light Imager, luminograph LB 981, EG&G Berthold, Bad Wildbad, Germany) was a high-performance low-light imaging system which is able to detect any type of luminescent emission (400–600 nm) over a wide range of intensities. It is designed for macroimaging of *in vivo* gene expression in tissues or whole organisms, and for the simultaneous measurement of multiple samples in microplates with its highest sensitivity comparable to that of luminometers *in vitro* (38). The analytical performance of the NightOWL was sufficiently evaluated for application to the quantitative detection of ultralow-light CL in terms of background, sample size, geometry, sensitivity, resolution, accuracy, and precision (38). The NightOWL slow-scan CCD camera was a peltier-air-cooled camera (−73°C) for ultralow-light imaging with a high sensitivity, the resolution being defined by 385 × 578 pixels. The luminescent signals on a photocathode in the image intensifier were detected as photons. The system was controlled by a DOS/V personal computer (OS: Micsosoft Windows 95) provided with software for quantitative image analysis. The whole instrument was installed in an air-conditioned room (24°C and 35% relative humidity).

Measurements of chemiluminescence in mouse skin. The hair on the back of a mouse was shaved with hair clippers, and its stratum corneum was carefully stripped with a commercially available depilatory (Shiseido, Tokyo, Japan). The bald mouse was used in the experiment 24 h after depilation treatment. The mouse was anesthetized by intraperitoneal injection of pentobarbital (50 mg kg^{-1} body weight), fixed on a black polystyrene 96 well microplate, covered with black cloth on which two circles with the same area (1260 pixels = 1.50×10^{-3} mm^2) were cut, and placed in a light-tight box to prevent interference by external light. The measured areas were divided into two parts (right and left sides in the mouse back skin) for comparative investigation. For the detection of spontaneous and UVA-induced ROS in each mouse, one area in mouse skin was treated with UVA irradiation and the other was left without treatment. Skin areas of the live mouse were exposed to UVA irradiation (320–400 nm) for 1 min through a UVA filter and a flexible fiber at a dose of 800 mW cm^{-2} generated with a Supercure-203S (San-Ei Electric MFG, Osaka, Japan). During UVA exposure, the anesthetized mouse remained under the detector. 5 μl of 400 μM CLA solution dissolved in H_2O was applied to the two circles on the mouse back skin immediately after UVA irradiation. Measurement of the light emission due to the *in vivo* CL began 30 s following the application of CLA to the skin. Identification of ROS and the ability of topical applications containing SOD (62.5 μM in H_2O), CAT (20 μM in H_2O), β-carotene (10 mM in 50% ethanol), and DFO (2 mM in H_2O) were examined, in which each 5 μl of ROS scavengers or a chelating agent and vehicle was applied to the treated and untreated skin before UVA irradiation, respectively. No effects of each vehicle on the

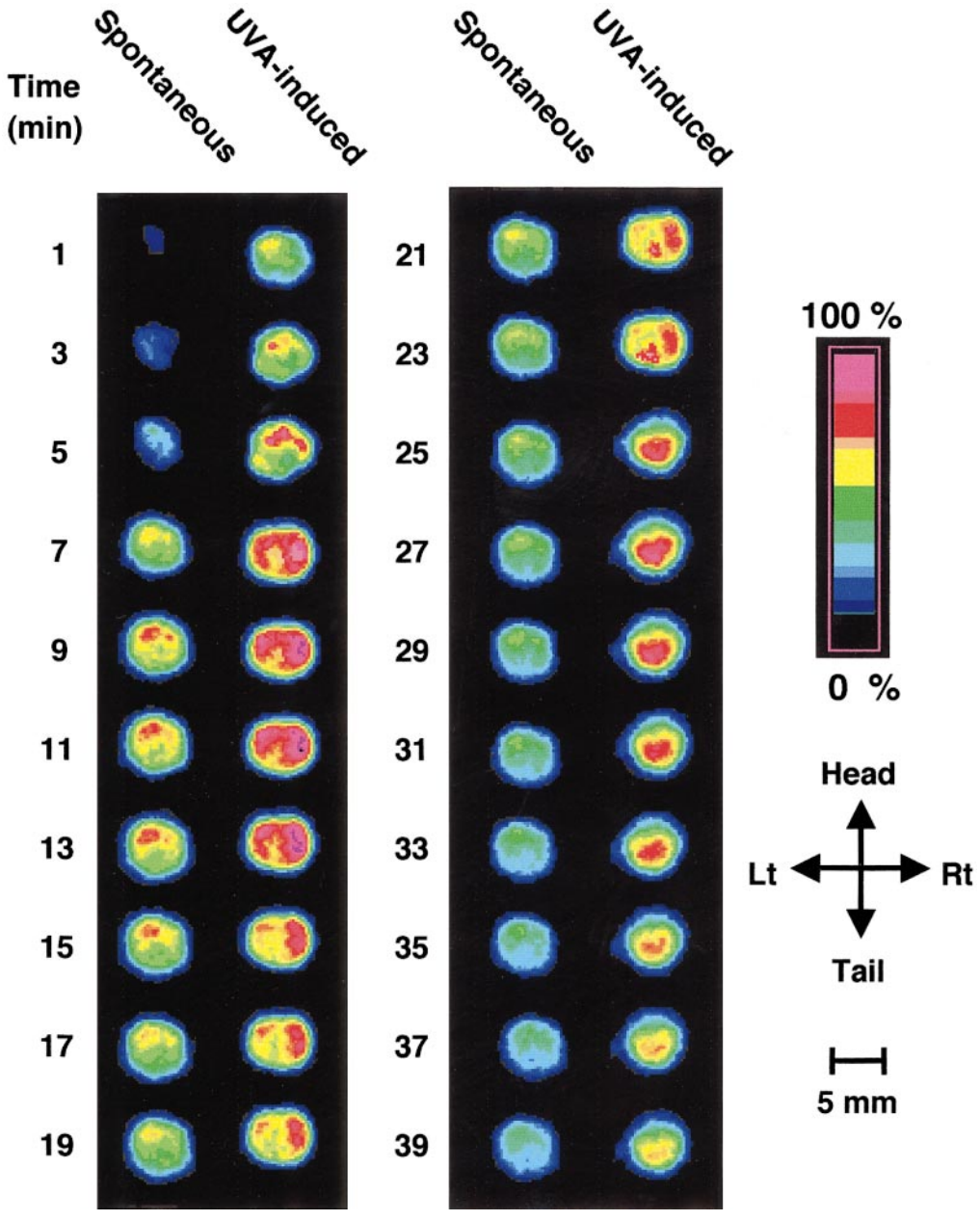

FIG. 1. Typical visualization and quantification of the *in vivo* chemiluminescent signals in mouse skin due to $^{\bullet}O_2^-$ and/or $^1O_2$ using CLA as the chemiluminescent probe. Each light emission image was acquired using the NightOWL imaging system with the following instrument settings: exposure time, 1 min; pixel size, 2 × 2; no background subtraction; camera readout slow. Pseudo-color displays of different chemiluminescent signals were obtained from normal and UVA-exposed mouse skin. Pseudo-color ruler on the right shows the relative light intensity.

measurements were confirmed in advance. The light emitted from the sample was accumulated for 1 min and integrated for 2 s on the camera tube's target at 1-min intervals for 40 min, which was sufficient to gather acceptable light emission data. The light emission output was then recorded on a memory device. The image was processed with a nonlinear gray scale to modify the contrast. A pseudo-color function converted the different gray shades to the colors. The quantification was expressed as the measurement of light from a single given area (1260 pixels = 1.50×10^{-3} mm^2). The background was calculated for the black cloth over the mouse with a signal/noise ratio of ≥3 considered as the detection limit. The results were expressed as photons s^{-1} pixel^{-1} (means ± standard deviations, numbers of mice = 3 or 4).

RESULTS AND DISCUSSION

An image of spontaneous and UVA-induced CL produced directly in a mouse skin *in vivo* was time-dependent, as shown with a pseudo-color function in Fig. 1. The hair-depilated mouse covered with the

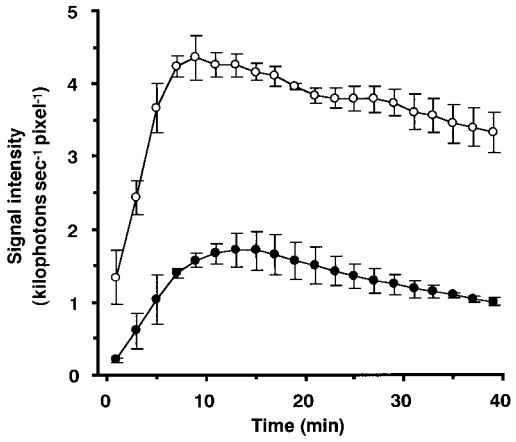

FIG. 2. Time-dependent profiles of the chemiluminescent signal intensities using CLA as the chemiluminescent probe. Light emission signal intensities were expressed as photons s^{-1} $pixel^{-1}$. The background values of signal intensities in the black cloth were subtracted from the measured values of those in the skin of live mice. Instrumental conditions were the same as those in Fig. 1. The signal intensities were due to spontaneous (●) and UVA-induced (○) chemiluminescence. Data were expressed as means ± standard deviations (numbers of mice = 4).

black cloth was a suitable model for the evaluation of the spatial resolution and quantitative aspects of the ultralow-light imaging, since the background could be quantified simultaneously with the photon emission derived from the black cloth. Similar areas located within the black cloth provided the mean background values, and the mean photon emission derived from mouse skin was significantly higher than the background value. The imaging data indicated that the single photon could be imaged as the single light spot, the spatial information could be shown in the image directly, and that a clear difference existed between UVA-treated and untreated skin areas. In Fig. 1, the UVA-irradiated skin exhibited significantly higher CL (right side) than did normal skin (left side), indicating the increased oxidative processes in the skin.

In addition to the spatial information, this imaging system provided further information regarding the time courses of the CL signal intensities in the mouse skin (Fig. 2). The signal intensities of light emission were quantitatively calculated in circular areas located on mouse back skin (1260 pixels = 1.50×10^{-3} mm^2), and those averaged values with standard deviations for four mice were shown in Fig. 2. Clearly increased curves of the CL signal intensities after UVA stimulation were obtained from each original source image. The reported data indicate the extraordinary ability of CL imaging to evaluate the spatial distribution of CL signals created by ROS which were generated spontaneously or UVA stimulatively in mouse skin, as well as to quantitatively analyze these signals.

Since a significant difference was observed between spontaneous and UVA-induced CL in mouse skin, the kinds of ROS could be identified by using topical applications containing typical and specific ROS scavengers and a chelating agent. Applications containing SOD or β-carotene were found to greatly reduce UVA-induced CL in the skin (Figs. 3b and 3d). Furthermore, SOD also highly reduced spontaneous skin CL (Fig. 3a), while β-carotene hardly reduced it (Fig. 3c). On the other hand, CAT, deferoxamine, and SOD denatured by boiling showed no ability to reduce either spontaneous or UVA-induced skin CL (data not shown). Therefore, the facts that SOD is a potent $^1O_2$ quencher (quenching rate constant = 2.6×10^9 M^{-1} s^{-1}) as well as an $^{\cdot}O_2^-$ scavenger (second-order rate constant = 2.0×10^9 M^{-1} s^{-1}) (20, 40) and β-carotene is a typical $^1O_2$ quencher (quenching rate constant = $3–30 \times 10^9$ M^{-1} s^{-1}) (40) suggest that the spontaneous CL was due mostly to $^{\cdot}O_2^-$, and that the UVA-induced CL was due predominantly to $^1O_2$ in mouse skin. It is recently demonstrated in an *in vivo* study that $^1O_2$ generated from a photosensitization reaction modifies CAT (41), and that the increase of mitochondrial common deletion in photoaged skin is attributable to the generation of $^1O_2$ (42). Thus, several studies have suggested that $^1O_2$ generation after UVA excitation in the skin results in UVA-induced photoaging of the skin (41–43). We demonstrated here the first direct *in vivo* evidence for the spontaneous occurrence of $^{\cdot}O_2^-$ and the UVA-induced formation of $^1O_2$ endogenously generated in mouse skin.

Both the location and the real-time development of the *in vivo* CL due to $^{\cdot}O_2^-$ and/or $^1O_2$ were directly observed, by means of supersensitive two-dimensional ultralow-light luminographs. The emitted light from differing skin sites to which various treatments had been applied could be analyzed both simultaneously and quantitatively. These results show the possibility of performing quantitative imaging at the tissue level and suggest analytical challenges for other applications. The measurement of novel two-dimensional CL directly from mouse skin has the advantage of being noninvasive and providing convenient and continuous monitoring. This method constitutes a unique *in vivo* tool for skin research, especially with regard to the detection of oxidative stress processes and the evaluation of antioxidants for the skin. To the best of our knowledge, the time- and space-dependent dynamics of the CL signals from mouse skin *in vivo* have not been previously reported. This spatial information is very important in understanding the mechanism and biological function of endogenously generated ROS, especially with regard to the investigation of skin response to UV-ray stress.

The new technique proposed here will determine the kinetics of endogenously generated ROS, and provide

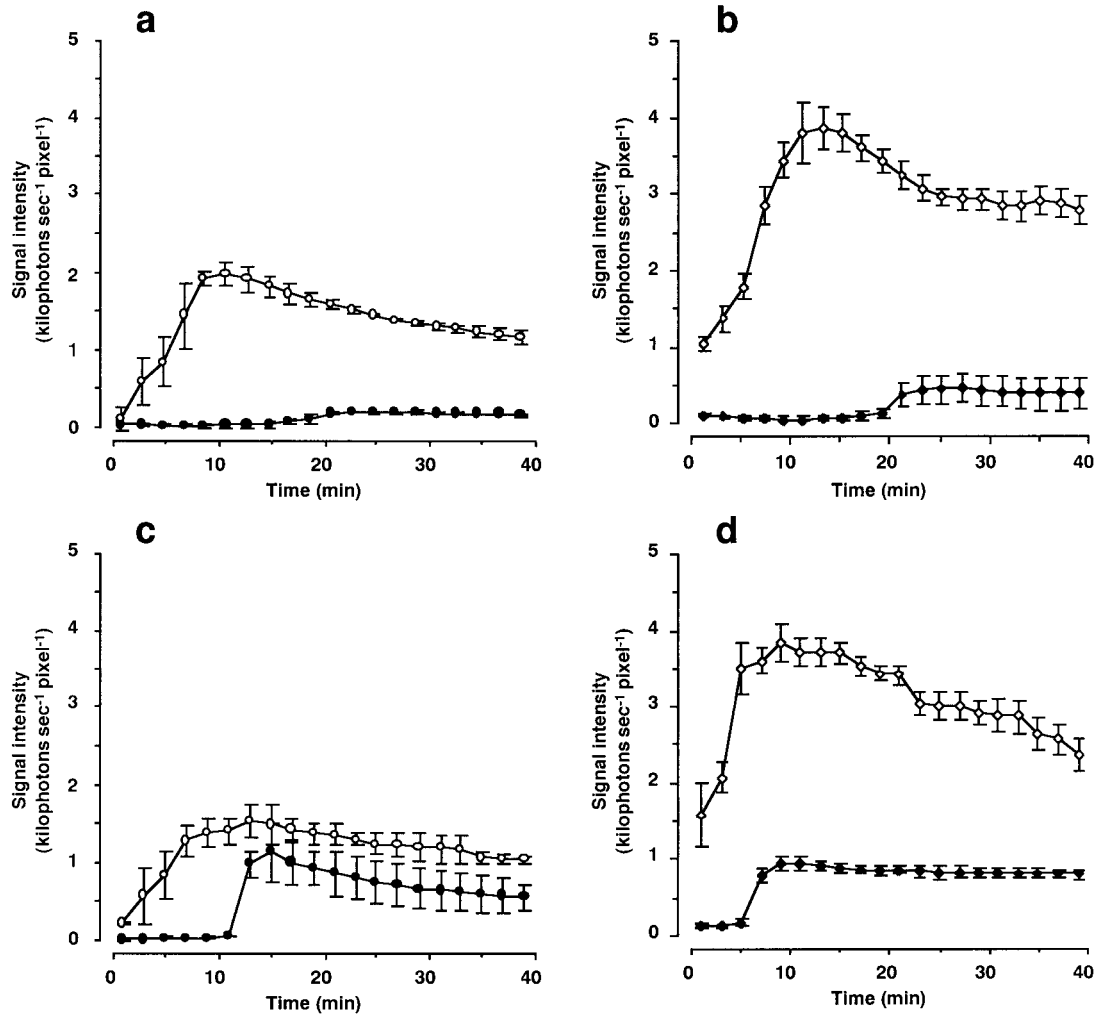

FIG. 3. Comparison of reactive oxygen species (ROS) and the protective effects of SOD and β-carotene on spontaneous and UVA-induced chemiluminescence generated in mouse skin. 5 μl of SOD (62.5 μM in H_2O) or β-carotene (10 mM in 50% ethanol) was topically applied to the treated skin before UVA irradiation. (a) Spontaneous signals without treatment (○) and with treatment of SOD (●), (b) UVA-induced signals without treatment (◇) and with treatment of SOD (◆), (c) spontaneous signals without treatment (○) and with treatment of β-carotene (●), (d) UVA-induced signals without treatment (◇) and with treatment of β-carotene (◆). Data were expressed as means ± standard deviations (numbers of mice = 3 in each experiment).

the simple, convenient, and convincing evaluation of the protective effects of antioxidant and photoprotective agents on UV-induced oxidative stress and other free radical processes.

ACKNOWLEDGMENTS

We are thankful to Mr. Satoshi Yoshida (EG&G Berthold) for his great technical support. This work has been supported in part by a grant from the Ministry of Science, Education, Sports and Culture of Japan to H.S.

REFERENCES

1. Kerr, J. B., and McElroy, C. T. (1993) *Science* **262,** 1032–1034.
2. Sudo, N., Takeshita, S., Sakata, T., and Sasaki, M. (1993) *Photomed. Photobiol.* **15,** 147–148.
3. Bruls, W. A., Slaper, H., van der Leun, J. C., and Berrens, L. (1984) *Photochem. Photobiol.* **40,** 485–494.
4. Sato, Y. (1991) *in* Photosensitive Dermatoses, pp. 3–17, 2nd ed., Kanehara, Tokyo.
5. Kligman, A. M. (1969). *J. Am. Med. Assoc.* **210,** 2377–2380.
6. Oikarinen, A., Karvonen, J., Uitto, J., and Hannuksela, M. (1985) *Photodermatology* **2,** 15–26.
7. Bech-Thomsen, N., and Wulf, H. C. (1995) *Photochem. Photobiol.* **62,** 773–779.
8. Nishi, J., Ogura, R., Sugiyama, M., Hidaka, T., and Kohno, M. (1991) *J. Invest. Dermatol.* **97,** 115–119.
9. Masaki, H., Atsumi, T., and Sakurai, H. (1995) *Biochem. Biophys. Res. Commun.* **206,** 474–479.
10. Masaki, H., and Sakurai, H. (1997) *J. Dermatol. Sci.* **14,** 207–216.
11. Tyrrell, R. M., and Pidoux, M. (1989) *Photochem. Photobiol.* **49,** 407–412.

12. Berneburg, M., Grether-Beck, S., Kurten, V., Ruzicka, T., Briviba, K., Sies, H., and Krutmann, J. (1999) *J. Biol. Chem.* **274,** 15345–15349.
13. Miyachi, Y., Horio, T., and Imamura, S. (1983) *Clin. Exp. Dermatol.* **8,** 305–310.
14. Masaki, H., Okano, Y., and Sakurai, H. (1998) *Arch. Dermatol. Res.* **290,** 113–118.
15. Plastow, S. R., Lovell, C. R., and Young, A. R. (1987) *J. Invest. Dermatol.* **88,** 145–148.
16. Hanada, K., Gange, R. W., and Connor, M. J. (1991) *J. Invest. Dermatol.* **96,** 838–840.
17. Yamazaki, S., Ozawa, N., Hiratsuka, A., and Watabe, T. (1999) *Free Radical Biol. Med.* **27,** 301–308.
18. Evelson, P., Ordonez, C. P., Llesuy, S., and Boveris, A. (1997) *J. Photochem. Photobiol. B* **38,** 215–219.
19. Sauermann, G., Mei, W. P., Hoppe, U., Stäb, F. (1999) *Methods Enzymol.* **300,** 419–428.
20. Rotilio, G., Bray, R. C., and Fielden, E. M. (1972) *Biochim. Biophys. Acta* **268,** 605–609.
21. Khan, A. V. (1976) *J. Phys. Chem.* **80,** 2219–2228.
22. Gal, D. (1994) *Biochem. Biophys. Res. Commun.* **202,** 10–16.
23. Tawa, R., and Sakurai, H. (1997) *Anal. Lett.* **30,** 2811–2825.
24. Arima, Y., Hatanaka, A., Tsukihara, S., Fujimoto, K., Fukuda, K., and Sakurai, H. (1997) *Chem. Pharm. Bull.* **45,** 1881–1886.
25. Masaki, H., Okano, Y., and Sakurai, H. (1997) *Biochem. Biophys. Res. Commun.* **235,** 306–310.
26. Hino, T., Kawanishi, S., Yasui, H., and Sakurai, H., (1998) *Biochim. Biophys. Acta* **1425,** 47–60.
27. Masaki, H., Okano, Y., and Sakurai, H. (1999) *Biochim. Biophys. Acta* **1428,** 45–56.
28. Osada, M., Ogura, Y., Yasui, H., and Sakurai, H. (1999) *Biochem. Biophys. Res. Commun.* **263,** 392–397.
29. Goto, T., and Takagi, T. (1980) *Bull. Chem. Soc. Jpn.* **53,** 833–834.
30. Nakano, M., Sugioka, K., Ushijima, Y., and Goto, T. (1986) *Anal. Biochem.* **159,** 363–369.
31. Sugioka, K., Nakano, M., Kurashige, S., Akuzawa, Y., and Goto, T. (1986) *FEBS Lett.* **197,** 27–30.
32. Nakano, M., Kimura, H., Hara, M., Kuroiwa, M., Kato, M., Totsune, K., and Yoshikawa T. (1990) *Anal. Biochem.* **187,** 277–280.
33. Sakurai, T., Sugioka, K., and Nakano, M. (1990) *Biochim. Biophys. Acta* **1043,** 27–33.
34. Koga, S. Nakano, M., and Uehara, K. (1991) *Arch. Biochem. Biophys.* **289,** 223–229.
35. Uehara, K., Maruyama, N., Huang, C. K., and Nakano, M. (1993) *FEBS Lett.* **335,** 167–170.
36. Hooper, C. E., Ansorge, R. E., Browne, H. M., and Tomkins, P. (1990) *J. Biolumin. Chemilumin.* **5,** 123–130.
37. Nicolas, J. C. (1994) *J. Biolumin. Chemilumin.* **9,** 139–144.
38. Roda, A., Pasini, P., Musiani, M., Girotti, S., Baraldini, M., Carrea, G., and Suozzi, A. (1996) *Anal. Chem.* **68,** 1073–1080.
39. Stawinska, D., and Stawinski, J. (1998) *J. Biolumin. Chemilumin.* **13,** 21–24.
40. Bellus, D. (1979) *Adv. Photochem.* **11,** 105–205.
41. Lledias, F., Rangel, P., and Hansberg, W. (1998) *J. Biol. Chem.* **273,** 10630–10637.
42. Berneburg, M., Grether-Beck, S., Kürten, V., Ruzicka, T., Briviba, K., Sies, H., and Krutmann, J. (1999) *J. Biol. Chem.* **274,** 15345–15349.
43. Hanson, K. M., and Simon, J. D. (1998) *Proc. Natl. Acad. Sci. USA* **95,** 10576–10578.